

## Article

# Impact of Hillslope Agriculture on Soil Compaction and Seasonal Water Dynamics in a Temperate Vineyard

Jasmina Defterdarović <sup>1,\*</sup> , Lana Filipović <sup>1</sup> , Gabrijel Ondrašek <sup>1</sup> , Igor Bogunović <sup>2</sup> , Ivan Dugan <sup>2</sup> , Vinod Phogat <sup>3,4,5</sup> , Hailong He <sup>6,7</sup> , Mehran Rezaei Rashti <sup>8</sup> , Ehsan Tavakkoli <sup>4</sup> , Thomas Baumgartl <sup>9</sup> , Abolfazl Baghbani <sup>10</sup> , Timothy I. McLaren <sup>11</sup>  and Vilim Filipović <sup>1,11,\*</sup> 

- <sup>1</sup> Department of Soil Amelioration, Division for Agroecology, Faculty of Agriculture, University of Zagreb, 10000 Zagreb, Croatia; lfipovic@agr.hr (L.F.); gondrasek@agr.hr (G.O.)
  - <sup>2</sup> Department of General Agronomy, Division for Agroecology, Faculty of Agriculture, University of Zagreb, 10000 Zagreb, Croatia; ibogunovic@agr.hr (I.B.); idugan@agr.hr (I.D.)
  - <sup>3</sup> Crop Sciences, South Australian Research and Development Institute, GPO Box 397, Adelaide, SA 5001, Australia; vinod.phogat@adelaide.edu.au
  - <sup>4</sup> School of Agriculture, Food and Wine, The University of Adelaide, PMB No.1, Glen Osmond, Urrbrae, SA 5064, Australia; ehsan.tavakkoli@adelaide.edu.au
  - <sup>5</sup> College of Science and Engineering, Flinders University, Adelaide, SA 5042, Australia
  - <sup>6</sup> College of Natural Resources and Environment, Northwest A&F University, Yangling 712100, China; hailong.he@hotmail.com
  - <sup>7</sup> Department of Soil Science, University of Manitoba, Winnipeg, MB R3T 2N2, Canada
  - <sup>8</sup> Australia Rivers Institute and School of Environment and Science, Griffith University, Nathan, QLD 4111, Australia; m.rezaeirashiti@griffith.edu.au
  - <sup>9</sup> Future Regions Research Centre, Geotechnical and Hydrogeological Engineering Research Group, Federation University, Latrobe, VIC 3841, Australia; t.baumgartl@federation.edu.au
  - <sup>10</sup> Department of Engineering, La Trobe University, Melbourne, VIC 3086, Australia; abaghbani@deakin.edu.au
  - <sup>11</sup> School of Agriculture and Food Sustainability, The University of Queensland, St Lucia, QLD 4072, Australia; tim.mclaren@uq.edu.au
- \* Correspondence: jdefterdarovic@agr.hr (J.D.); v.filipovic@uq.edu.au (V.F.)



**Citation:** Defterdarović, J.; Filipović, L.; Ondrašek, G.; Bogunović, I.; Dugan, I.; Phogat, V.; He, H.; Rashti, M.R.; Tavakkoli, E.; Baumgartl, T.; et al. Impact of Hillslope Agriculture on Soil Compaction and Seasonal Water Dynamics in a Temperate Vineyard. *Land* **2024**, *13*, 588. <https://doi.org/10.3390/land13050588>

Academic Editor: Víctor Fernández-García

Received: 26 March 2024  
Revised: 24 April 2024  
Accepted: 26 April 2024  
Published: 28 April 2024



**Copyright:** © 2024 by the authors. Licensee MDPI, Basel, Switzerland. This article is an open access article distributed under the terms and conditions of the Creative Commons Attribution (CC BY) license (<https://creativecommons.org/licenses/by/4.0/>).

**Abstract:** Major losses of agricultural production and soils are caused by erosion, which is especially pronounced on hillslopes due to specific hydrological processes and heterogeneity. Therefore, the aim of this study was to assess the impact of agricultural management on the compaction, infiltration, and seasonal water content dynamics of the hillslope. Measurements were made at the hilltop and footslope, i.e., soil water content and potential were measured using sensors, wick lysimeters were used to quantify water flux, while a mini-disk infiltrometer was used to measure the infiltration rate and calculate the unsaturated hydraulic conductivity ( $K_{unsat}$ ). Soil texture showed differences between hillslope positions, i.e., at the hilltop after 50 cm depth, the soil is classified as silty clay loam, and from 75 cm onward, the soil is silty clay, while at the footslope, the soil is silt loam even at the deeper depths. The results show a higher  $K_{unsat}$  at the footslope as well as higher average water volumes collected in wick lysimeters compared to the hilltop. Average water volumes showed a statistically significant difference at  $p < 0.01$  between the hilltop and the footslope. The soil water content and water potential sensors showed higher values at the footslope at all depths, i.e., 8.0% at 15 cm, 8.4% at 30 cm, and 27.3% at 45 cm. The results show that, even though the vineyard is located in a relatively small area, soil heterogeneity is present, affecting the water flow along the hillslope. This suggests the importance of observing water movement in the soil, especially today when facing extreme weather (e.g., short-term high-intensity rainfall events) in order to protect soil and water resources.

**Keywords:** hillslope; infiltration; sensors; wick lysimeters; compaction

## 1. Introduction

Agricultural production on hillslopes is challenging due to land degradation caused by tillage and soil erosion, which accordingly leads to soil heterogeneity and various specific hydrological processes, e.g., surface runoff, subsurface preferential and lateral flows, and chemical processes caused by a change in the equilibrium state [1–4]. However, such locations are frequently used for horticultural production, e.g., vineyards, because of their favorable properties, like sun exposure and the lack of waterlogging or mist formation.

The complexity of hillslope soils is noticeable in the additional processes that occur compared to plain soils, such as soil erosion, subsurface preferential lateral flow, surface runoff, etc. These processes affect water flow, and thus the transport of pollutants (fertilizers, pesticides, etc.) and water balance on the hillslope. Therefore, the knowledge of hydrological processes in such soils is essential for sustainable water and soil management. Furthermore, soil erosion on the hillslope is caused by surface runoff, soil tillage, as well as trafficking in general, resulting in subsurface compaction causing increased soil strength, which consequently has negative impacts on root development, plant nutrient uptake, and reduced soil aeration and hydraulic conductivity [5–7]. These processes also lead to a greater soil physical heterogeneity along the hillslope. As a result, upper positions have a less permeable layer closer to the surface compared to the lower ones, eventually affecting the water balance and resulting in a reduced hydraulic conductivity that can lead either to lateral subsurface flow or surface runoff. Subsequently, lateral subsurface flow can occur in arable soils at the tillage depth where a compacted horizon (e.g., plow pan or hard pan) is present [8].

The presence and volume of lateral subsurface flow firstly depend on the precipitation intensity and amount. Furthermore, differences in hydraulic properties, especially hydraulic conductivity, can appear as a result of various soil layers and impact lateral subsurface flow. Additionally, other characteristics influencing lateral subsurface flow are soil depth, hillslope angle, antecedent moisture condition, and the physical characteristics of the preferential flow network [9,10]. As a result, preferential flow occurs bypassing most of the soil solid phase and causing relatively faster fluxes compared to the other types of flow in the vadose zone [11]. Previous studies [12] suggested that pedologically identical soil horizons do not always have identical soil hydraulic properties as a result of a different slope position, depth of soil development, and parent material. On the other hand, it is important to consider the soil infiltration rate as one of the factors that has a direct impact on runoff [13], leaching, and crop water availability, leading to an easier prediction of surface runoff [14].

Understanding the soil infiltration rate is important for sustainable management. While it must be considered when draining and/or irrigating, it affects solutes' transport, groundwater recharge, and ecosystem sustainability. According to Morbidelli et al. [15], the infiltration rate decreases as the slope increases as a result of a reduced available time for rainfall infiltration. In spite of the larger complexity and less predictability compared to the flow under saturated conditions, unsaturated hydraulic conductivity can be calculated using infiltration rates measured by a mini-disk infiltrometer (MDI), among other methods. An MDI is based on the principle of a tension infiltrometer, where the macropores with an air entry value smaller than the suction of the infiltrometer are eliminated. The applied water under tension or suction does not enter into the macropores, e.g., cracks and wormholes, but it is affected by hydraulic forces in the soil and is drawn through the finer pores of the soil [16]. The MDI is a widely used method for the determination of infiltration rates and hydraulic conductivity both in the field (e.g., [17–19]) and in the laboratory (e.g., [20,21]).

The objective of this study was to (i) assess the effect of agricultural management (i.e., trafficking) on compaction, infiltration, and seasonal water content dynamics along the hillslope and (ii) to determine if there are any differences between the hilltop and the footslope. Therefore, to determine the water flow behavior on the hillslope, we combined several methods, i.e., the estimation of soil hydraulic parameters (SHPs), sensor-based measurement of soil water content and water potential, quantifying water flux using

wick lysimeters, measuring infiltration using a MDI, and calculating the water potential-associated unsaturated hydraulic conductivity. The research was conducted at the hilltop and the footslope, and the results collected at these positions are compared. Combining several methods, this study aimed to gain more precise insights into hillslope hydrology and the effect of compaction closer to the surface on the upper position compared to the lower ones as a result of soil erosion. Since the study was conducted during summer months, the effects of short-term high-intensity rainfall events were also investigated. Understanding these processes will consequently lead to better agricultural practices in the future.

## 2. Materials and Methods

### 2.1. Study Location and Soil Properties

The study was conducted at the Experimental Station Jazbina ( $45^{\circ}51'21.1''$  N,  $16^{\circ}00'10.0''$  E; Figure 1) in Zagreb, Croatia, as a preliminary study for the first Croatian critical zone observatory (Suprehill). Ploughing, pesticides and fertilizer application, as well as the collection of the grapes are managed by the Department of Viticulture and Enology, UNIZG-AGR. The vineyard soil is affected by these trafficking practices as the passing lines are on a downslope and are repeated every year.

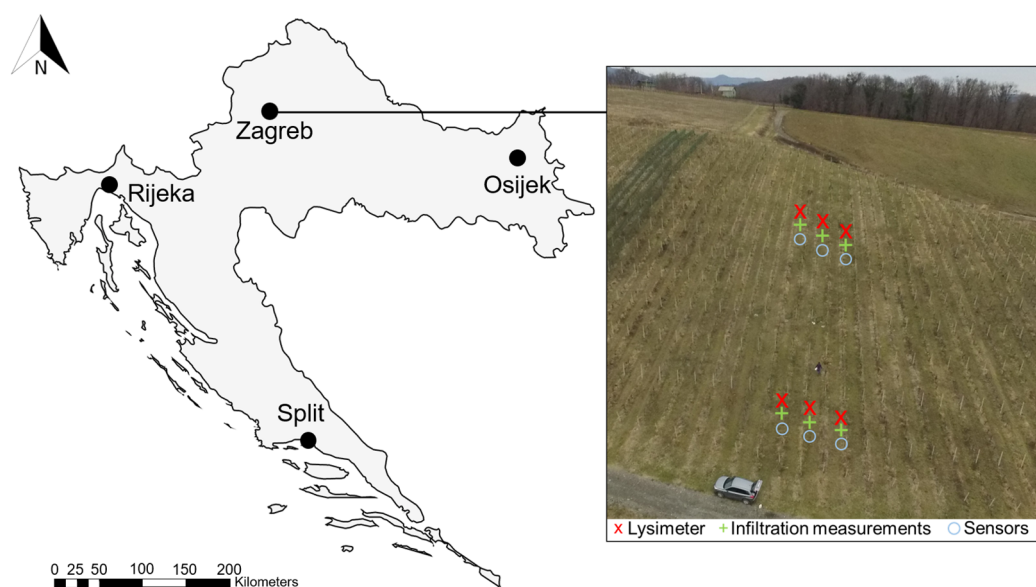


**Figure 1.** Study location in Croatia and positions of lysimeters (red), infiltration measurements (green), and sensors (blue) set on the hilltop and the footslope with a slope angle of 20%.

According to the world reference base for soil resources, the soil at Jazbina is classified as a Luvic Stagnosol (IUSS Working Group WRB, 2022) [22]. The vineyard is located on a slope of 20% and the interrow area is grassed. The long-term (50 years) average annual temperature is  $11.2^{\circ}\text{C}$ , while the average annual precipitation is 856.5 mm. Figure 2 shows the precipitation (a) and temperature (b) measured at the investigated hillslope from December 2017 to December 2018.

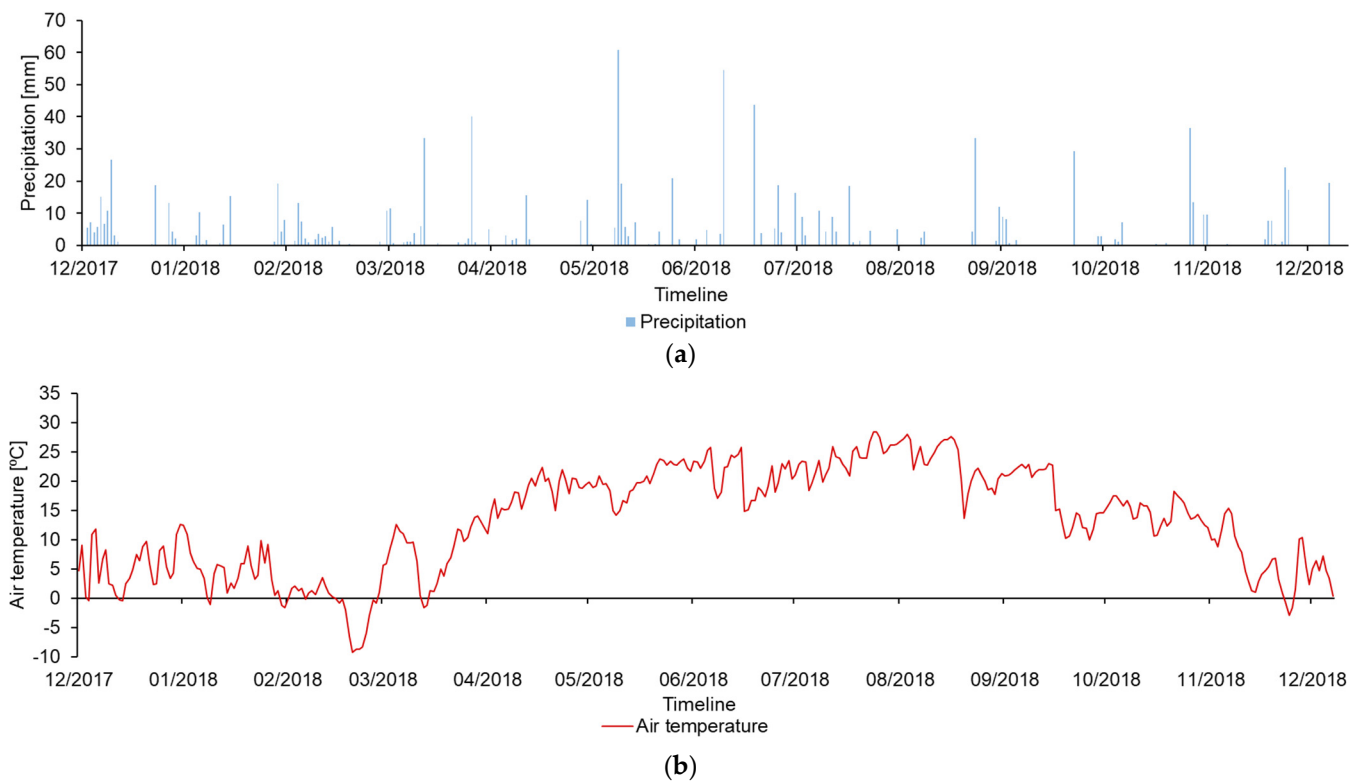


**Figure 2.** (a) Precipitation (mm) and (b) daily air temperature (°C) measured by the meteorological station at the investigated site from December 2017 to December 2018.

Disturbed soil samples were taken at the hilltop and the footslope of the investigated location at five depths (0–15, 15–30, 30–50, 50–75, and 75–100 cm) in three replicates. Samples were analyzed for texture, pH, electrical conductivity (E.C.), and organic carbon ( $C_{org}$ ). Disturbed sample preparation was performed by the standardized method [23]. Soil particle size distribution was determined by sieving and sedimentation [24], and texture classes were determined according to USDA. Furthermore, the soil pH and E.C. were determined by the standardized method [25,26], and organic carbon by sulfochromic oxidation [27].

## 2.2. Soil Hydraulic Parameters' Estimation

Undisturbed soil cores ( $250 \text{ cm}^3$ ) were taken in three replicates at the hilltop and the footslope at a depth ranging from 5 to 10 cm. At the footslope, one replicate was excluded due to the large macropores present inside the cylinder. The soil hydraulic parameters (SHPs) were estimated using the undisturbed soil cores ( $250 \text{ cm}^3$ ) using the simplified evaporation method [28] and the HYPROP automated system, which is applicable to most soil types [29]. Two tensiometers were placed at predefined positions inside the undisturbed soil samples at two depths to measure the soil water tension during the drying process [30]. The analysis based on the Wind's method uses the water suctions measurements to derive the hydrological parameters. The fitting quality for the soil hydraulic parameters estimation is expressed in terms of the root-mean-square error (RMSE), which indicates the mean distance between a data point and the fitted function [31].  $R^2$  is a coefficient of determination used as a fitting parameter for soil hydraulic parameters as well.

SHPs were derived using the van Genuchten model (vG) [32]:

$$\begin{aligned} \theta(h) &= \theta_r + \frac{\theta_s - \theta_r}{(1 + |\alpha h|^n)^m} \text{ for } h < 0 \\ \theta(h) &= \theta_s \text{ for } h \geq 0 \end{aligned} \quad (1)$$

$$K(h) = K_s S_e^l \left( 1 - \left( 1 - S_e^{\frac{1}{m}} \right)^m \right)^2 \quad (2)$$

$$S_e = \frac{\theta - \theta_r}{\theta_s - \theta_r} \quad (3)$$

$$m = 1 - \frac{1}{n} \quad n > 1 \quad (4)$$

where  $\theta_r$  and  $\theta_s$  denote the residual and saturated volumetric water contents ( $\text{cm}^3 \text{cm}^{-3}$ ), respectively;  $h$  is the pressure head;  $S_e$  is the effective saturation (-);  $\alpha$  ( $\text{cm}^{-1}$ ) and  $n$  (-) are the shape parameters; and  $l$  (-) is a pore connectivity parameter. The pore connectivity parameter,  $l$ , was fixed to a value of 0.5, as recommended for most soils [33].

### 2.3. Infiltration Measurements

The soil infiltration rates were measured on the field using a MDI. Figure 3 shows the infiltration rate measurement using the MDI at the hilltop and its features. The unsaturated hydraulic conductivity was calculated via a Microsoft Excel spreadsheet provided by the manufacturer *Decagon* (Decagon Devices, Pullman, WA, USA). The soil infiltration measurements were conducted at two depths, i.e., 5 and 25 cm, in three replicates (one replicate per row) and at the hilltop and the footslope using the MDI with a suction head varying from 1 to 5 cm. The SWC was measured at the hilltop and the footslope right before the infiltration measurements close to the MDI. The infiltration measurements were performed between May and June 2018.

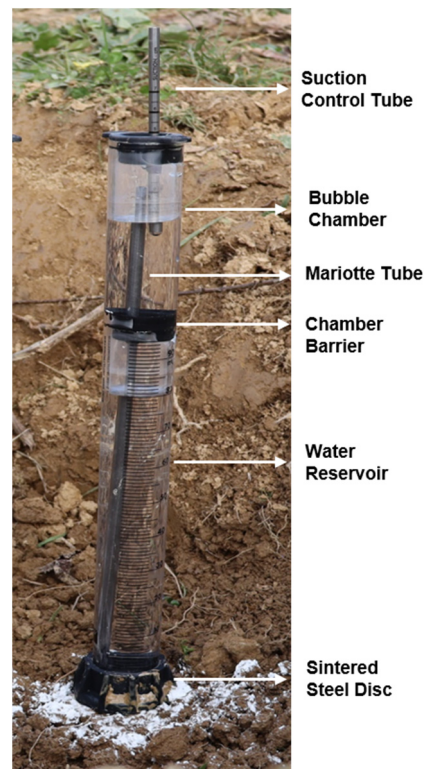


**Figure 3.** Field infiltration measurement using a mini-disk infiltrometer (MDI) at a 25 cm depth at the hilltop of the investigated location, with applied quartz sand on the soil surface to ensure better contact.

At the beginning of the infiltration measurements, the grass was removed from the soil surface and quartz sand was applied to ensure a better contact between the infiltrometer and the soil. Briefly, when the infiltrometer is placed on the soil surface, water from the

lower chamber begins to flow and infiltrate into the soil, which is related to the hydraulic properties of the soil [16].

The infiltration is calculated according to the equation proposed by Zhang et al. [34], which requires measuring the cumulative infiltration versus time and fitting the results with the function:

$$I = C_1 t + C_2 \sqrt{t} \quad (5)$$

where  $C_1$  ( $\text{m s}^{-1}$ ) and  $C_2$  ( $\text{m s}^{-1/2}$ ) are parameters.  $C_1$  is related to hydraulic conductivity, and  $C_2$  is the soil sorptivity. The hydraulic conductivity of the soil ( $k$ ) is then computed from:

$$k = \frac{C_1}{A} \quad (6)$$

where  $C_1$  is the slope of the curve of the cumulative infiltration vs. the square root of time, and  $A$  is a value relating the van Genuchten parameters for a given soil type to the suction rate and radius of the infiltrometer disk.  $A$  is computed from:

$$A = \frac{11.65(n^{0.1} - 1) \exp[2.92(n - 1.9)\alpha h_0]}{(\alpha r_0)^{0.91}} n \geq 1.9 \quad (7)$$

$$A = \frac{11.65(n^{0.1} - 1) \exp[7.5(n - 1.9)\alpha h_0]}{(\alpha r_0)^{0.91}} n < 1.9 \quad (8)$$

where  $n$  and  $\alpha$  are the van Genuchten parameters for the soil,  $r_0$  is the disk radius, and  $h_0$  is the suction at the disk surface.

#### 2.4. Determination of the Water Flow Using Lysimeters and Sensors

Zero tension lysimeters were set up at the field (Figure 4), three at the top of the hillslope and three at the footslope. The lysimeters were round with 50 cm in diameter, and inserted into the soil at a 40 cm depth with disturbed soil from the same location within. The bottom of the lysimeter was connected via a rubber tube to a container in which the leachate was collected and sampled after rainfall events during the period from December 2017 to July 2018. The statistical analysis of collected data was performed using the SAS software (Statistical Analysis Software, SAS Institute Inc., Cary, NC, USA, Version 4.3, 2006). For the water volume, an analysis of variance was performed using a one-way ANOVA with the lysimeter position as the independent variable only, and also with data grouping according to the sampling date. Significant differences between the means were determined using Tukey's HSD (honestly significant difference) test at  $p < 0.01$ .



**Figure 4.** Setting up of the zero tension lysimeters (50 cm in diameter) at the hilltop and the footslope at a 40 cm depth.

Soil water content (SWC) sensors (GS-1, METER) were installed at two depths—15 and 30 cm—while soil water potential (SWP) sensors (MPS-6, METER) were installed at a 45 cm depth. Both GS-1 and MPS-6 sensors were set at the hilltop and the footslope. SWC and SWP measurements were taken from 16 May 2018 to 13 December 2018.

### 3. Results

#### 3.1. Physical and Chemical Characteristics

Table 1 shows the soil physical and chemical characteristics of the investigated location. Figure 5 shows the particle size distribution at the hilltop and the footslope of the investigated location. The less permeable layer occurs at 50 cm at the hilltop, where the texture class changes from silt loam to silty clay loam. The clay content also increased, and at a 75–100 cm depth, it is 40%, changing the texture class to silty clay. Furthermore, it can be seen that  $C_{org}$  is higher at the hilltop compared to the footslope at the first two depths, while at 30–50 cm, it is the same. At a 50 cm depth,  $C_{org}$  is higher at the footslope compared to the hilltop. Also, at a 50 cm depth, differences in the soil particle size are more pronounced, not only for the clay but also for the sand and silt.

**Table 1.** Physical and chemical characteristics at the hilltop and the footslope of the investigated location at depths of 0–15, 15–30, 30–50, 50–75, and 75–100 cm.

Position	Depth (cm)	Soil Particle Size Distribution (%)			Texture Classes (USDA)	pH (H <sub>2</sub> O)	E.C. (dS m <sup>-3</sup> )	C <sub>org</sub> (g kg <sup>-1</sup> )
		Sand	Silt	Clay				
Hilltop	0–15	12	69	19	Silt loam	6.56	0.054	17.29
	15–30	10	68	22	Silt loam	6.18	0.041	11.72
	30–50	11	64	25	Silt loam	5.97	0.047	8.06
	50–75	12	55	33	Silty clay loam	5.79	0.058	5.80
	75–100	18	42	40	Silty clay	5.60	0.083	3.07
Footslope	0–15	7	68	25	Silt loam	6.94	0.049	12.18
	15–30	9	64	27	Silty clay loam	7.07	0.048	8.70
	30–50	8	69	23	Silt loam	6.87	0.038	8.06
	50–75	7	70	23	Silt loam	6.51	0.051	7.89
	75–100	6	69	25	Silt loam	5.09	0.058	4.93

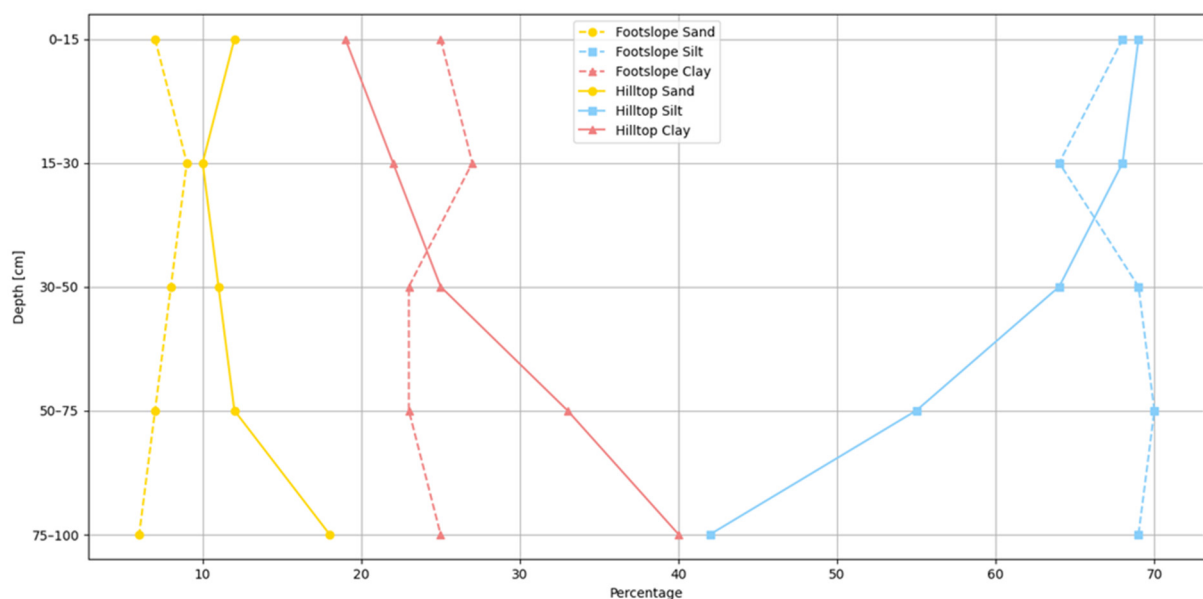


**Figure 5.** Soil particle size distribution at the hilltop and the footslope of the investigated hillslope at depths of 0–15, 15–30, 30–50, 50–75, and 75–100 cm.

### 3.2. Soil Hydraulic Parameters' Estimation

SHPs (Table 2) as well as soil water retention curves (Figure 6) were estimated and obtained using the HYPROP-FIT program [31]. The estimated water content in the soil under fully saturated conditions ( $\theta_s$ ) was higher at the top of the hillslope. Saturated hydraulic conductivity ( $K_s$ ) was slightly higher at the hilltop; however, it was very low at both positions. The estimated bulk density and porosity were  $1.3 \text{ g cm}^{-3}$  and 51%, respectively, at the hilltop and  $1.22 \text{ g cm}^{-3}$  and 54%, respectively, at the footslope.

**Table 2.** van Genuchten (vG) hydraulic parameters calculated by HYPROP-FIT for the hilltop and the footslope. The  $\theta$  value represents the water content,  $\alpha$  and  $n$  are shape parameters, and  $K$  represents the hydraulic conductivity.  $RMSE$  and  $R^2$  indicate the van Genuchten (vG) model fit with the measured data.

Hillslope Position	Sampling Depth (cm)	$\theta_r$ ( $\text{cm}^3 \text{ cm}^{-3}$ )	$\theta_s$ ( $\text{cm}^3 \text{ cm}^{-3}$ )	$\alpha$ ( $\text{l cm}^{-1}$ )	$n$	$K_s$ ( $\text{cm day}^{-1}$ )	$RMSE_\theta$	$RMSE_K$	$R^2_\theta$	$R^2_K$
Hilltop	5–10	0.000 *	0.491	0.0078	1.15	1.82	0.0379	0.6646	0.9953	0.9994
Footslope	5–10	0.000 *	0.302	0.0061	1.22	0.457	0.0212	0.4061	0.9924	0.9993

\* model assumption;  $\theta_r$  values are close to 0.

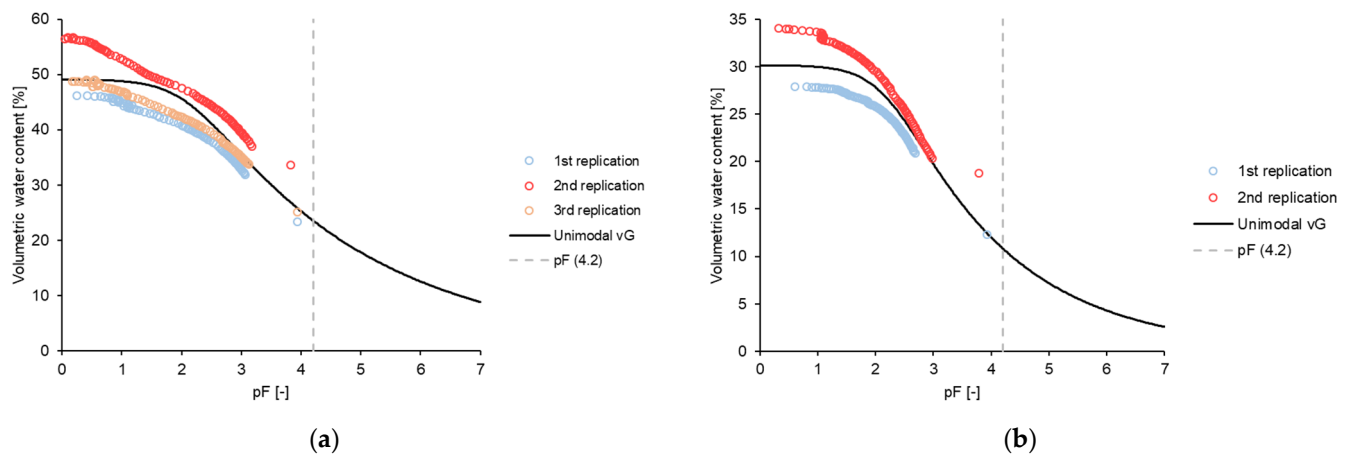


**Figure 6.** Soil water retention curves obtained using the HYPROP-FIT program for (a) the hilltop and (b) the footslope (5–10 cm) using the van Genuchten (vG) unimodal model.

### 3.3. Infiltration Measurements

The unsaturated hydraulic conductivity ( $K_{unsat}$ ) was measured at the hilltop and the footslope at the two depths of  $-5$  and  $25$  cm. Table 3 and Figures A1–A4 show  $K_{unsat}$  at different suctions obtained using the provided Microsoft Excel spreadsheet (by the MDI manufacturer *Decagon*).  $K_{unsat}$  varied at each position depending on the applied suction rate (from  $-1$  to  $-5$  cm). At the hilltop, the values ranged from  $7.85$  to  $42.26 \text{ cm day}^{-1}$ , and at the depth of  $25$  cm, from  $2.58$  to  $9.75 \text{ cm day}^{-1}$ . The values at the footslope were higher and ranged from  $8.89$  to  $47.33 \text{ cm day}^{-1}$ , and at a  $25$  cm depth, from  $4.40$  to  $18.85 \text{ cm day}^{-1}$ . The water content values before the infiltration measurement at the  $5$  cm depth were  $13.41\%$  for the hilltop and  $14.24\%$  for the footslope. At a  $25$  cm depth, these values were  $19.43\%$  for the hilltop and  $31.81\%$  for the footslope. Even though the SWC was not the same at the hilltop and the footslope, infiltration measurements were conducted because these were real field conditions and the goal was to investigate how the water infiltrates into the soil if precipitation occurs.

**Table 3.** Soil hydraulic conductivity ( $K_{unsat}$ ) at different suction rates measured using the mini-disk infiltrometer (MDI) at the hilltop and footslope at 5 and 25 cm depths in three replicates.

Hillslope Position	Depth (cm)	Suction Rate (cm)				
		−1	−2	−3	−4	−5
		Hydraulic Conductivity (cm day <sup>−1</sup> )				
Hilltop	5	42.26	33.24	14.89	18.30	7.85
	25	9.75	6.83	4.94	3.60	2.58
Footslope	5	47.33	39.58	23.02	19.56	8.89
	25	18.85	13.01	9.56	8.80	4.40

### 3.4. Determination of the Water Flow Using Lysimeters and Sensors

The precipitation and water volumes for each sampling date are shown in Figure 7. For the period from 7 December 2017 to 23 July 2018, the average water volume at the hilltop was 1.7 L and, at the footslope, 4.0 L, which shows a statistically significant difference at  $p < 0.01$ .

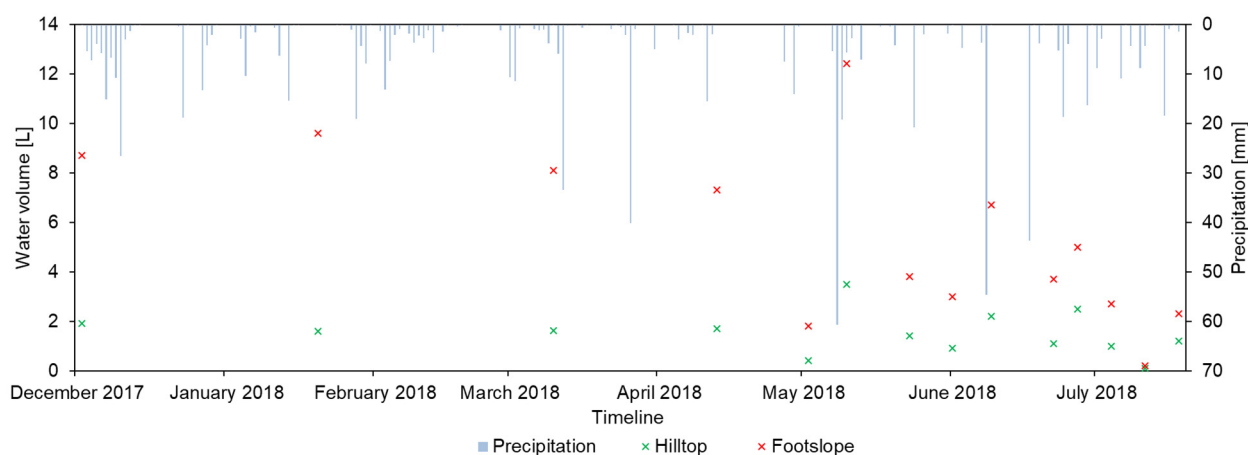


**Figure 7.** Water volume collected in the wick lysimeter at the hilltop and the footslope on different sampling dates during the period from December 2017 to July 2018 with the precipitation rate.

The water volumes collected with the footslope lysimeter are higher compared to the volumes collected with the hilltop lysimeter on almost every sampling date (it was the same on 2 July and 16 July, and negligibly lower on 23 July 2018). From 7 December 2017 to 18 April 2018 and on 15 May 2018, the water volume at the footslope was significantly higher compared to that at the hilltop.

The SWC was measured at two depths (15 and 30 cm) at the hilltop and the footslope and is shown in Figures 8 and 9, depending on the precipitation. At the top of the hillslope at a depth of 15 cm, the SWC varied from 0.150 to 0.359  $\text{m}^3 \text{m}^{-3}$ , with average values of 0.266  $\text{m}^3 \text{m}^{-3}$ . At the same position but at a 30 cm depth, the SWC varied from 0.218 to 0.399  $\text{m}^3 \text{m}^{-3}$  (average of 0.308  $\text{m}^3 \text{m}^{-3}$ ), which presents on average a 13.64% increase. Furthermore, the SWP (Figure 10) at a 45 cm depth varied from  $-9.79$  to  $-5164$  kPa. On the other hand, at the footslope at a depth of 15 cm, the SWC varied from 0.181 to 0.399  $\text{m}^3 \text{m}^{-3}$ , with average values of 0.289  $\text{m}^3 \text{m}^{-3}$ , and at a 30 cm depth, from 0.285 to 0.392  $\text{m}^3 \text{m}^{-3}$  (average 0.336  $\text{m}^3 \text{m}^{-3}$ ), which present on average an increase of 13.99%. Moreover, at a 45 cm depth, the SWP (Figure 10) varied from  $-10.40$  to  $-2846$  kPa. On average, the SWC on the footslope was 8.0% (15 cm), i.e., 8.4% (30 cm) greater than at the hilltop, and the SWP was also on average 27.3% greater at the footslope.

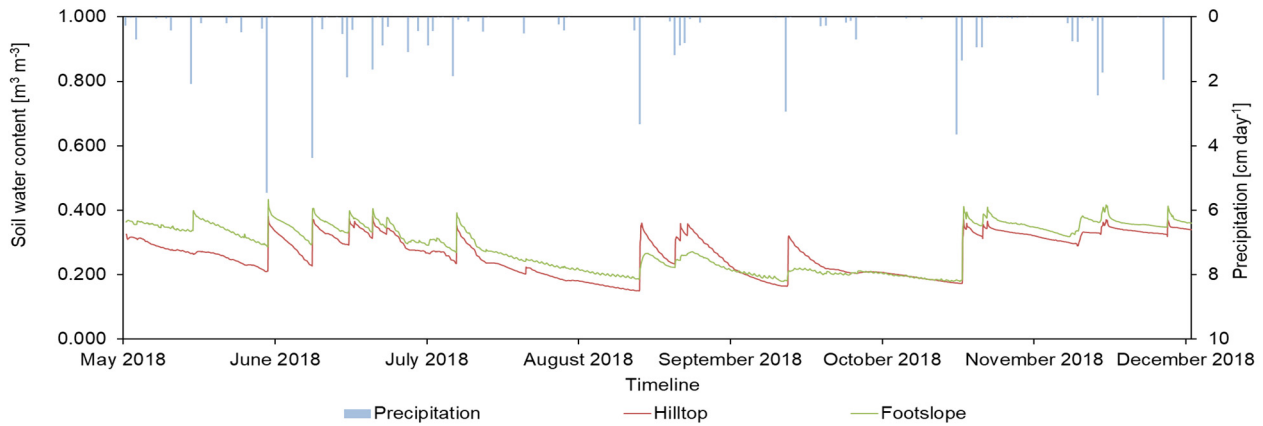


**Figure 8.** Soil water content (SWC) measurements depending on the precipitation on the hilltop and the footslope of the investigated hillslope at a 15 cm depth.

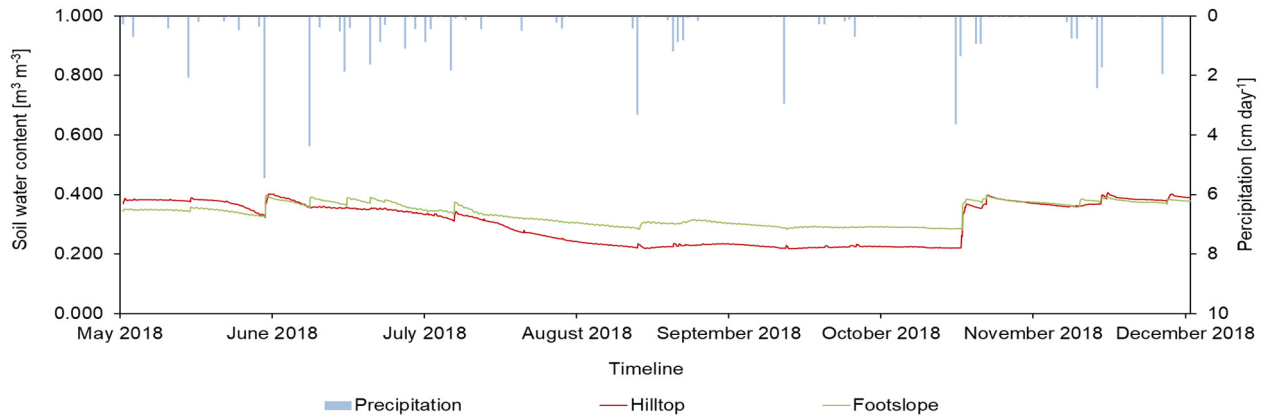


**Figure 9.** Soil water content (SWC) measurements depending on the precipitation on the hilltop and the footslope of the investigated hillslope at a 30 cm depth.

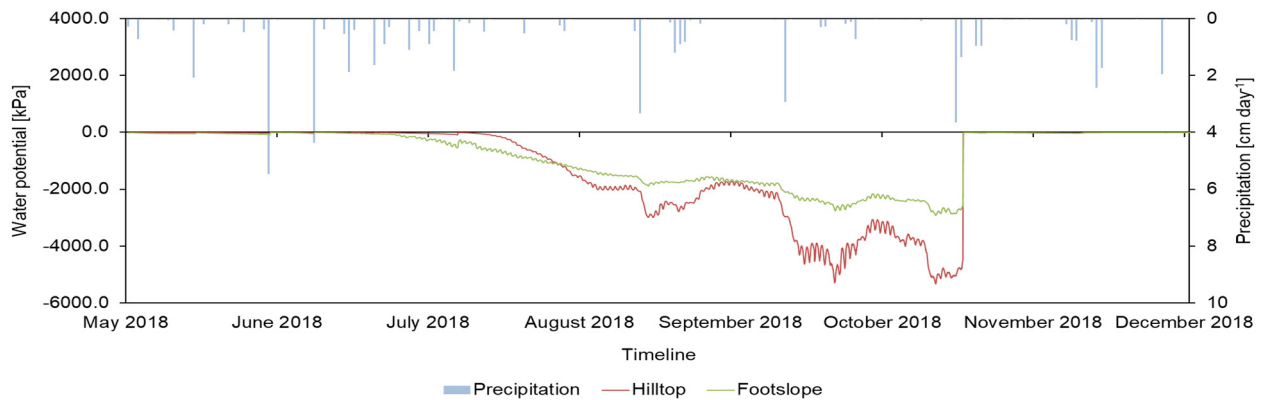


**Figure 10.** Soil water potential (SWP) measurements depending on the precipitation on the hilltop and the footslope of the investigated hillslope at a 45 cm depth.

It can be seen from Figures 8–10 that the largest response was obtained with sensors at a 15 cm depth. This was expected since it is the shallowest depth and it is under the influence of most factors (i.e., air temperature, wind, etc.). Sensors at a 15 cm depth also showed that the SWC was higher at the footslope for most of the year, except in the period from the end of August to the middle of September and then again from the end of September to the start of October. On the other hand, differences in the SWC at a depth of 30 cm between the hilltop and footslope were not that pronounced as well as differences

between drying and rewetting. Furthermore, according to SWP measurements, the soil was drying during the summer months, since there was not considerable precipitation, except for a few rainfall events, which were not enough to drastically rewet the soil, especially not at 45 cm. The SWP measurements showed that the soil was mostly drier at the hilltop compared to the footslope during the summer months and early autumn. On the contrary, during autumn, when the temperature and evaporation rate were lower, both hilltop and footslope SWP values were close to saturation.

## 4. Discussion

### 4.1. Physical, Chemical, and Hydraulic Characteristics

The topsoil had a better soil structure in general with a higher  $C_{org}$  content, lower bulk density, and higher porosity, resulting in more aerated conditions [35]. However, according to Figure 5, at the hilltop, the soil texture changes to a heavier silty clay loam and silty clay in the deeper layers (50–100 cm). This results in more pronounced compaction effects compared to the footslope. Additionally, the higher clay content in these layers exacerbates compaction, affecting the water flow in the subsurface and thus influencing the preferential flow and transport of applied chemicals, but also root penetration. Conversely, in the footslope, the soil remains predominantly as silt loam, even in the deeper layers. While compaction effects are still present, they are comparatively less severe than on the hilltop. Thus, in terms of agriculture, it can be assumed that roots in the footslope position may encounter less resistance, allowing for a relatively better penetration and exploration of the soil profile for water and nutrients. Furthermore, subsurface preferential lateral flow will not be that pronounced and more water will be present. The lower clay content in the deeper layers contributes to reduced compaction pressure compared to the hilltop. On the other hand,  $C_{org}$  is higher at a depth of 50–100 cm on the footslope, which also has decreasing effects on soil compaction [36]. Soil compaction poses distinct challenges to root growth and vegetation [37], but also changes water flow pathways in both hilltop and footslope positions, albeit with some differences based on the soil characteristics. Generally, a higher clay content typically leads to a greater compaction susceptibility.

The estimated bulk density was slightly higher on the hilltop compared to the footslope, while the porosity was slightly higher on the footslope. Furthermore, due to a low estimated  $K_s$  (HYPROP-FIT), surface runoff will occur, especially during high-intensity rainfall events, which are common in the summer.

### 4.2. Infiltration Measurements

The results show that, with the proximity to the less permeable layer, differences in  $K_{unsat}$  (MDI) between the hilltop and the footslope are more pronounced (2.58–9.75 cm day<sup>-1</sup> at the hilltop and 4.40–18.85 cm day<sup>-1</sup> at the footslope). This is a consequence of the change in texture class between the two hillslope positions. However, the footslope is silt loam even at the deeper depths; at the hilltop this changes at a depth of 50 cm. As mentioned above, at a depth of 50–75 cm at the hilltop, the soil texture changes to a heavier silty clay loam, and at a depth of 75–100 cm, to even heavier silty clay. This will result in surface runoff and thus soil erosion, which can eventually lead to the shallower depth of the less permeable layer at the hilltop. The differences are not that pronounced for the 5 cm depth measurements, due to the impact of more uniform conditions caused by grass cover and root activity (e.g., [38]). Roots modify the soil matrix and thus consequently influence the soil hydraulic conductivity, soil water storage, pore size distribution, and the connectivity between pores [39]. However, the topsoil is more exposed to the soil erosion caused by surface runoff, especially in the summer months with high-intensity rainfall events. These results are in line with those of other findings [40], which suggested that the surface layer was more affected by the slope gradient compared to the deeper layer since the slope gradient will determine the amount of surface runoff and the infiltration rate. Furthermore, although the depth distinction was only 20 cm, the differences between  $K_{unsat}$  measured with the MDI at a 5 and 25 cm depth were pronounced, suggesting soil heterogeneity and the impact of the proximity of the less

permeable layer, even in an arable horizon. In addition, the SWC before the infiltration measurement showed greater differences and higher values at the footslope (14.24% at a depth of 5 cm and 31.81% at a depth of 25 cm) compared to the hilltop (13.41% at a depth of 5 cm and 19.43% at a depth of 25 cm), especially at a depth of 25 cm. Since the measurements showed that the footslope had a higher SWC, this means that the slope position has an indirect impact on the infiltration measurements. This could be a result of soil erosion and a slightly higher amount of clay and a lower amount of sand compared to the top of the hillslope [41]. Additionally, the soil water repellency could be another reason for the higher  $K_{unsat}$  values at the footslope.  $C_{org}$  was higher at the hilltop position at a 0–30 cm depth (Table 1), which could cause higher water repellence and thus a lower infiltration rate [39,42]. Moreover, trafficking has a negative impact on the surface soil structural stability, which will be more pronounced on the hilltop due to the effects of the slope and thus soil erosion, causing less favorable soil water properties (e.g., [14]). This is also in line with the bulk density and porosity, where it is estimated that, at the footslope, the bulk density is slightly lower, while the porosity was slightly higher. Previous studies (e.g., [43,44]) suggest that the higher the bulk density, and the lower the porosity and the higher the soil compaction, which will affect the infiltration rate, i.e., it will be lower.

#### 4.3. Determination of the Water Flow Using Lysimeters and Sensors

The significant differences in collected water volumes in the lysimeters between the hillslope and the footslope were in line with most of the obtained results. Although HYPROP measurements showed that  $K_s$  was smaller at the footslope, the SWC and SWP showed that the footslope was wetter compared to the hilltop. Furthermore, the MDI showed that  $K_{unsat}$  was higher at the footslope, both at 5 and 25 cm depths. The estimated bulk density was lower at the footslope, and the total porosity was slightly higher. In the winter season, precipitation events are more long-lasting compared to those in the summer months, and the temperatures and the evapotranspiration rate are lower. Additionally, the soil hydrology is more favorable due to more frequent low-intensity precipitation, resulting in a higher soil water content. On the other hand, during the summer months, the temperatures and evapotranspiration rates are higher, and most of the precipitation is in the form of short-duration high-intensity rainfall events. These conditions would cause a lower SWC and soil water repellency, causing lower infiltration rates [45]. Since the study was conducted on the hillslope, this would cause less available time for infiltration [15], consequently causing a lower infiltration rate and thus higher surface runoff [46], nutrient losses, and preferential flow [45]. It can be seen from Figure 7 that the highest collected water volume was on the 15 May 2018, which was a result of the high-intensity rainfall events in that period causing a greater runoff. Güntner et al. [47] mentioned that the surface runoff formed at the hilltop positions could re-infiltrate in parts of the hillslope, in our case, at the footslope. Moreover, it is possible that, at the footslope, more biopores are present, resulting in a greater preferential flow. Due to soil erosion, a less permeable layer at the hilltop is closer to the surface, leading to a lower  $K_{unsat}$  at the upper positions and thus resulting in subsurface preferential lateral flow (e.g., [48]), resulting in more water at the footslope.

It is clear from Figures 8 and 9 that the SWC had a greater oscillation near the soil surface due to the faster sensors' response to the rainfall events as well as more intense drying by evaporation. Furthermore, an expected increase in the SWC can be noticed shortly after precipitation. On the other hand, at a 30 cm depth, oscillations in the SWC are less noticeable, especially in the summer period with a higher temperature and more drought events. Similarly, in terms of the SWC at a depth of 30 cm, the effect of a higher temperature and more high-intensity rainfall events resulted in surface runoff and caused a drastic decrease in the SWP values at a depth of 45 cm (Figure 10). As a result of the specified conditions in the summer months, which can cause soil water repellence (e.g., [49]) or soil crusting (e.g., [50]), it takes a longer time for the soil to infiltrate water, which can be seen as a lagged sensor's response after precipitation compared to the rainfall events

in other seasons. Additionally, in the deeper horizons, the sensors' response could be a result of subsurface runoff at the hillslope, especially when there is a less permeable layer (e.g., [8,11,51]). At the hilltop, oscillations at a 45 cm depth were greater compared to those at the footslope, and both drying and wetting were more pronounced. Figures 8–10 indicate that the first rainfall event that caused a greater sensors' response after the summer months was 28 October 2018. At a 15 cm depth, the sensors responded on the same day shortly after the rainfall; however, at a 45 cm depth, the sensors' response had the largest time delay.

A more pronounced water movement was observed at the footslope owing to the slight differences in the bulk density and total porosity, which can lead to differences in the water flow, i.e. macropores will cause increased water movement [35], or it could even be a result of preferential flows [8,11,48]. Furthermore, the surface runoff was more pronounced at the hilltop, resulting in a higher water volume at footslope positions. Considering all the above-mentioned reasons, the water from the whole hillslope would accumulate at the footslope, which was most pronounced in the winter period, i.e., in the period with greater precipitation and lower temperatures and evaporation rate.

## 5. Conclusions

The impact of hillslope agriculture on water dynamics was assessed using zero tension lysimeters, a mini-disk infiltrometer, soil water content, and potential sensors at various depths. The obtained results show an increased water flux at the footslope. The unsaturated hydraulic conductivity showed slightly higher values at the footslope at 5 and 25 cm depths compared to the hilltop with more pronounced differences at a 25 cm depth. Furthermore, the water volumes collected in the lysimeters on most sampling dates showed more water in this position. The average water volume was significantly higher at the footslope, which was the most pronounced in the period from 7 December 2017 to 18 April 2018 and on 15 May 2018. Finally, the results obtained using sensors show, on average, a higher water content and water potential values at the same position. The results show a higher water flow at the footslope, which could suggest a better pore connectivity. This is a consequence of heavier silty clay loam from 50 cm at the hilltop, ending in silty clay at 75 cm, which results in a higher soil compaction. Even though all the used methods showed similar results, the estimated  $K_s$  was very low at both hillslope positions and it was lower at the footslope. This could suggest that undisturbed samples were taken from even more compacted micro-locations (e.g., closer to the area underneath the tractor's wheel between the rows in the vineyard). However, by combining several various methods, a closer insight into water flow processes was established, and the impact of different events on water movement along the hillslope was investigated. All these results show the impacts of surface runoff and subsurface lateral flow on a water movement as well as the possible impact of the proximity of the less permeable layer caused by trafficking and soil erosion. It can be seen that the soil, and thus water flow heterogeneity, can be pronounced even on a relatively small area and cannot be generalized due to the number of affecting processes.

**Author Contributions:** Conceptualization, J.D. and V.F.; methodology, J.D., V.F. and L.F.; software, J.D., L.F. and V.F.; validation, J.D., L.F. and V.F.; formal analysis, J.D., L.F. and V.F.; investigation, G.O., I.B., I.D. and V.F.; resources, G.O.; data curation, J.D., L.F., G.O. and V.F.; writing—original draft preparation, J.D.; writing—review and editing, J.D., L.F., G.O., I.B., I.D., V.P., H.H., M.R.R., E.T., T.B., A.B., T.I.M. and V.F.; visualization, J.D. and A.B.; supervision, V.F.; project administration, G.O.; funding acquisition, G.O. All authors have read and agreed to the published version of the manuscript.

**Funding:** This research was funded by Hrvatske vode, grant number 10-059/17.

**Data Availability Statement:** Data are available upon request from the corresponding author. The data are not publicly available due to privacy.

**Acknowledgments:** We thank Vedran Krevh, Lorena Žabčić, and Filip Kranjčec for their help during the experiment.

**Conflicts of Interest:** The authors declare no conflicts of interest.

Appendix A

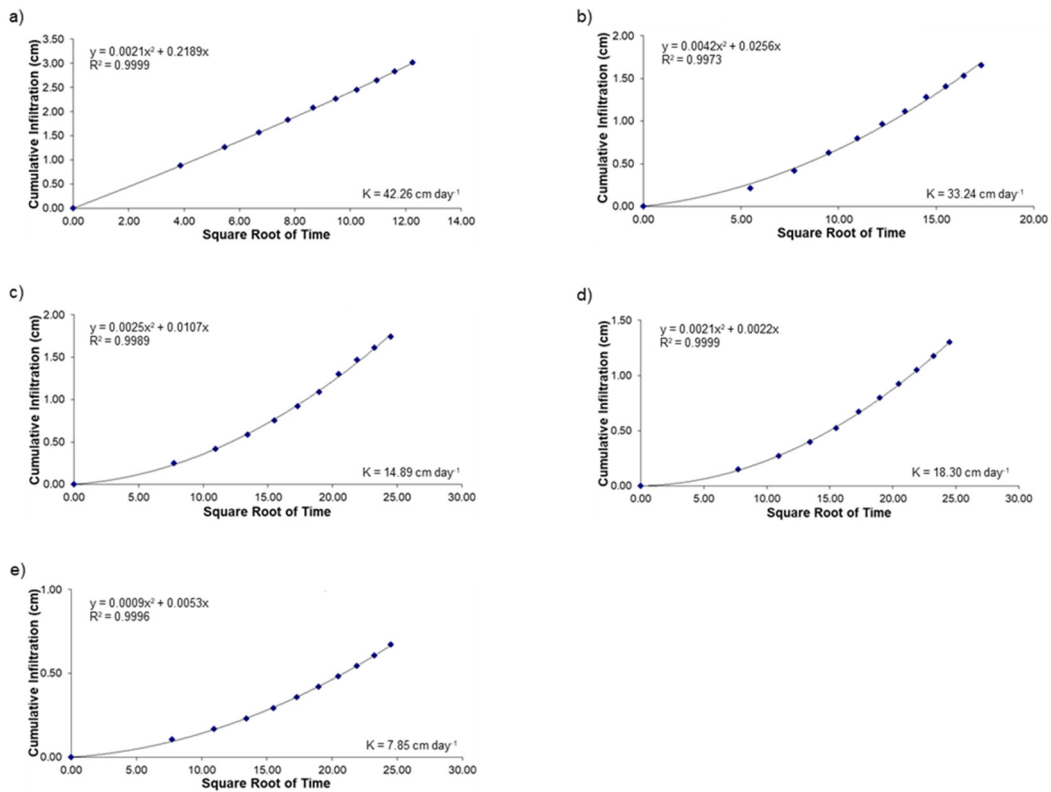


Figure A1. Soil hydraulic conductivity ( $K_{unsat}$ ) at different suction rates: (a) –1, (b) –2, (c) –3, (d) –4, and (e) –5 cm at the depth of 5 cm (hilltop).

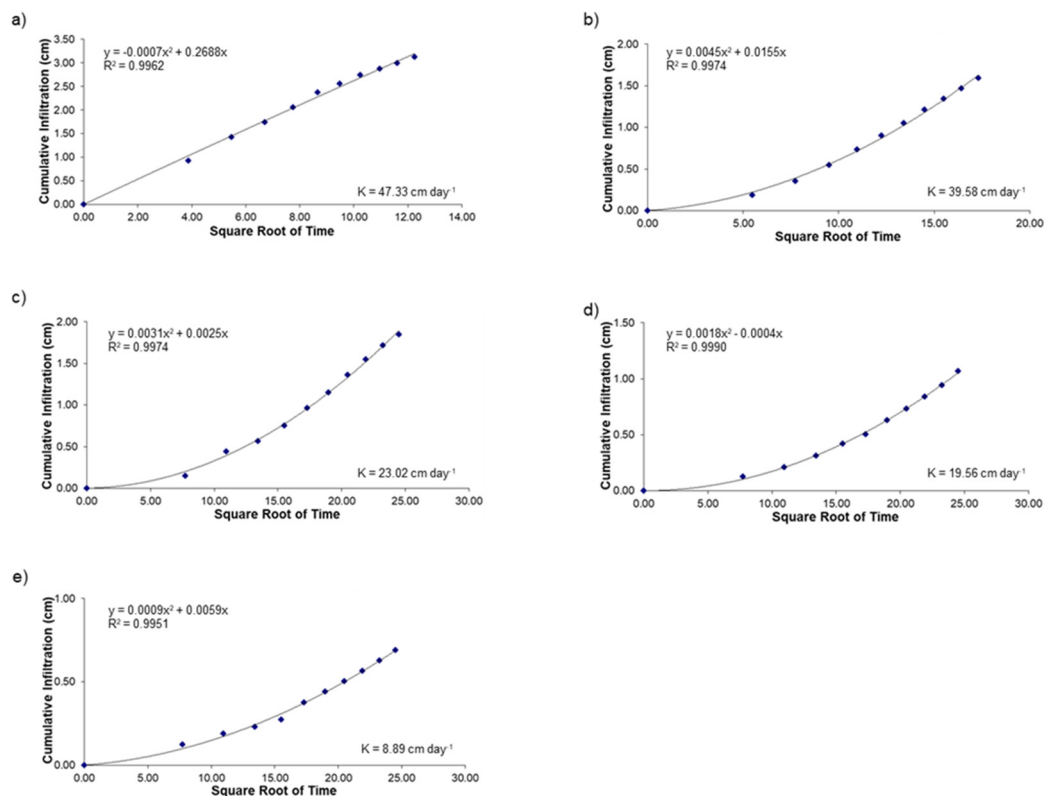
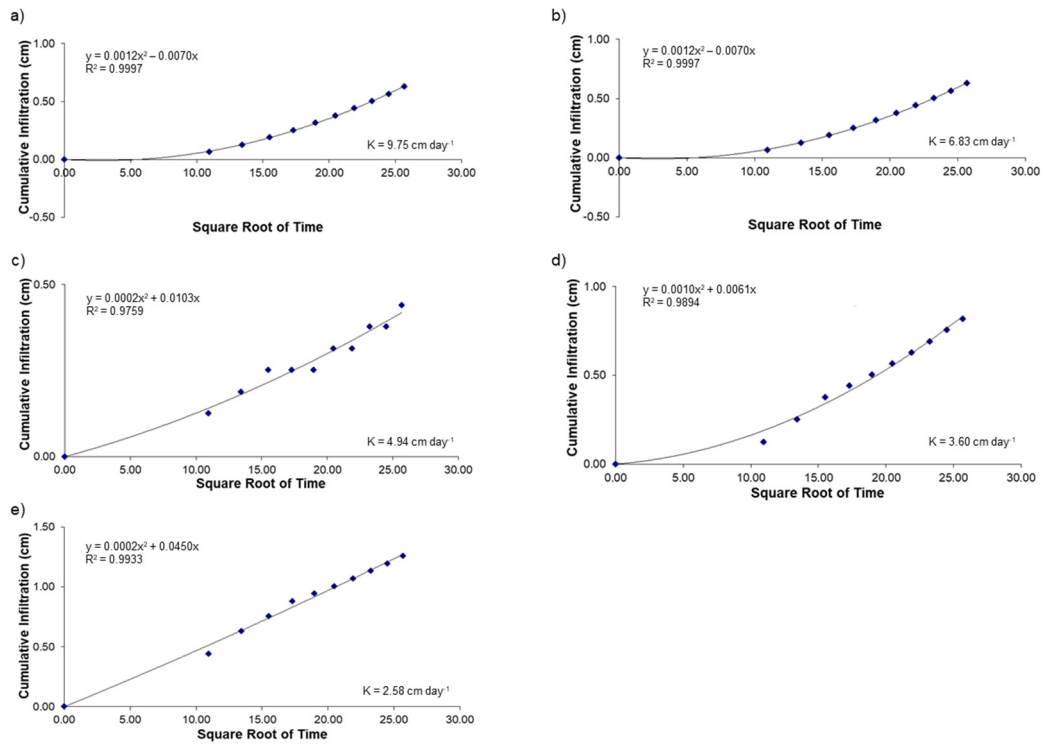
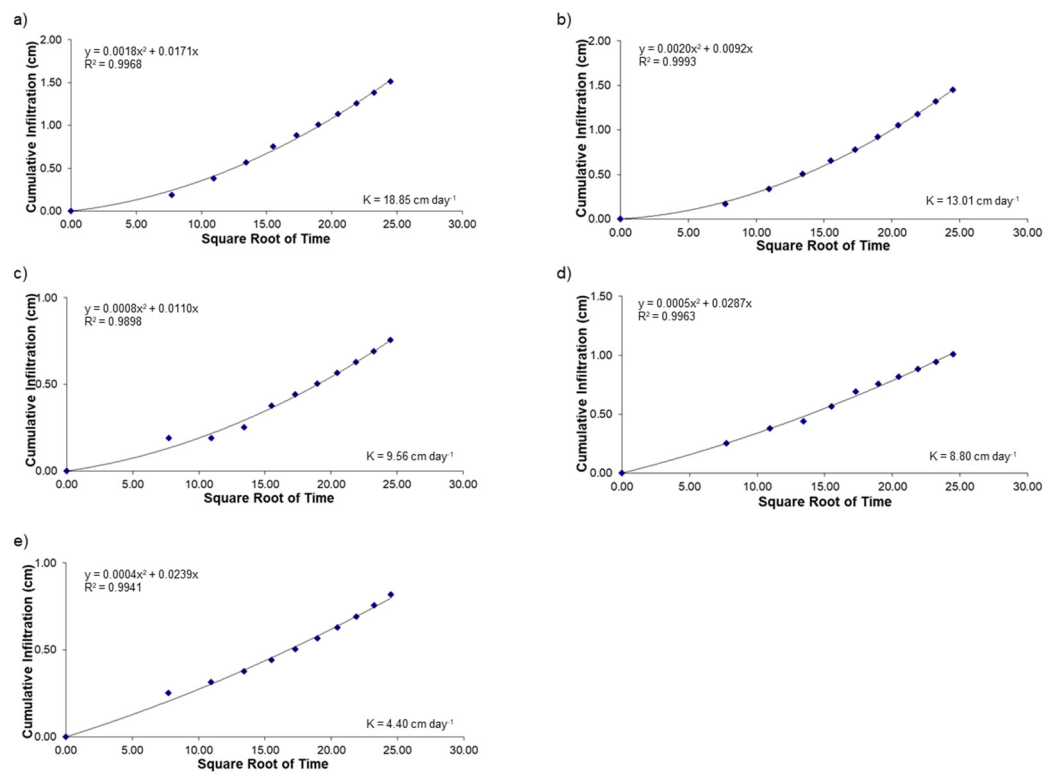


Figure A2. Soil hydraulic conductivity ( $K_{unsat}$ ) at different suction rates: (a) –1, (b) –2, (c) –3, (d) –4, and (e) –5 cm at the depth of 5 cm (footslope).



**Figure A3.** Soil hydraulic conductivity ( $K_{unsat}$ ) at different suction rates: (a) –1, (b) –2, (c) –3, (d) –4, and (e) –5 cm at the depth of 25 cm (hilltop).



**Figure A4.** Soil hydraulic conductivity ( $K_{unsat}$ ) at different suction rates: (a) –1, (b) –2, (c) –3, (d) –4, and (e) –5 cm at the depth of 25 cm (footslope).

## References

1. Apollonio, C.; Petroselli, A.; Tauro, F.; Cecconi, M.; Biscarini, C.; Zarotti, C.; Grimaldi, S. Hillslope Erosion Mitigation: An Experimental Proof of a Nature-based Solution. *Sustainability* **2021**, *13*, 6058. [CrossRef]
2. Cai, J.S.; Yan, E.C.; Yeh TC, J.; Zha, Y.Y. Effects of Heterogeneity Distribution on Hillslope Stability during Rainfalls. *Water Sci. Eng.* **2016**, *9*, 134–144. [CrossRef]
3. Filipović, V.; Gerke, H.H.; Filipović, L.; Sommer, M. Quantifying Subsurface Lateral Flow along Sloping Horizon Boundaries in Soil Profiles of a Hummocky Ground Moraine. *Vadose Zone J.* **2018**, *17*, 1–12. [CrossRef]
4. Nikodem, A.; Kodešová, R.; Fér, M.; Klement, A. Using Scaling Factors for Characterizing Spatial and Temporal Variability of Soil Hydraulic Properties of Topsoils in Areas Heavily Affected by Soil Erosion. *J. Hydrol.* **2021**, 593. [CrossRef]
5. Laker, M.C.; Nortjé, G.P. Review of Existing Knowledge on Subsurface Soil Compaction in South Africa. *Adv. Agron.* **2020**, *162*, 143–197. [CrossRef]
6. Raper, R.L. Agricultural Traffic Impacts on Soil. *J. Terramechan.* **2005**, *42*, 259–280. [CrossRef]
7. Mohammed, S.; Abdo, H.G.; Szabo, S.; Pham, Q.B.; Holb, I.J.; Linh, N.T.T.; Anh, D.T.; Alsafadi, K.; Mokhtar, A.; Kbibo, I.; et al. Estimating Human Impacts on Soil Erosion Considering Different Hillslope Inclinations and Land Uses in the Coastal Region of Syria. *Water* **2020**, *12*, 2786. [CrossRef]
8. Patil, M.D.; Das, B.S. Assessing the Effect of Puddling on Preferential Flow Processes through under Bund Area of Lowland Rice Field. *Soil Tillage Res.* **2013**, *134*, 61–71. [CrossRef]
9. Sørbotten, L.E.; Stolte, J.; Wang, Y.; Mulder, J. Hydrological Responses and Flow Pathways in an Acrisol on a Forested Hillslope with a Monsoonal Subtropical Climate. *Pedosphere* **2017**, *27*, 1037–1048. [CrossRef]
10. Anderson, A.E.; Weiler, M.; Alila, Y.; Hudson, R.O. Subsurface Flow Velocities in a Hillslope with Lateral Preferential Flow. *Water Resour. Res.* **2009**, *45*, W11407. [CrossRef]
11. Nimmo, J.R. The Processes of Preferential Flow in the Unsaturated Zone. *Soil Sci. Soc. Am. J.* **2021**, *85*, 1–27. [CrossRef]
12. Rieckh, H.; Gerke, H.H.; Sommer, M. Hydraulic Properties of Characteristic Horizons Depending on Relief Position and Structure in a Hummocky Glacial Soil Landscape. *Soil Tillage Res.* **2012**, *125*, 123–131. [CrossRef]
13. Cheremisinoff, N.P. Principles of Hydrogeology. In *Groundwater Remediation and Treatment Technologies*; William Andrew Publishing: Norwich, NY, USA, 1997; pp. 85–126. [CrossRef]
14. Franzluebbers, A.J. Water Infiltration and Soil Structure Related to Organic Matter and Its Stratification with Depth. *Soil Tillage Res.* **2002**, *66*, 197–205. [CrossRef]
15. Morbidelli, R.; Saltalippi, C.; Flammini, A.; Govindaraju, R.S. Role of Slope on Infiltration: A Review. *J. Hydrol.* **2018**, *557*, 878–886. [CrossRef]
16. Decagon Devices Inc. *Mini Disc Infiltrometer*; Decagon Devices Inc.: Pullman, WA, USA, 2016; pp. 1–20.
17. Naik, A.P.; Ghosh, B.; Pekkatt, S. Estimating Soil Hydraulic Properties Using Mini Disk Infiltrometer. *ISH J. Hydraul. Eng.* **2019**, *25*, 62–70. [CrossRef]
18. Radinja, M.; Vidmar, I.; Atanasova, N.; Mikoš, M.; Šraj, M. Determination of Spatial and Temporal Variability of Soil Hydraulic Conductivity for Urban Runoff Modelling. *Water* **2019**, *11*, 941. [CrossRef]
19. Bátková, K.; Miháliková, M.; Matula, S. Hydraulic Properties of a Cultivated Soil in Temperate Continental Climate Determined by Mini Disk Infiltrometer. *Water* **2020**, *12*, 843. [CrossRef]
20. Li, X.Y.; González, A.; Solé-Benet, A. Laboratory Methods for the Estimation of Infiltration Rate of Soil Crusts in the Tabernas Desert Badlands. *Catena* **2005**, *60*, 255–266. [CrossRef]
21. Soracco, C.G.; Villarreal, R.; Melani, E.M.; Oderiz, J.A.; Salazar, M.P.; Otero, M.F.; Irizar, A.B.; Lozano, L.A. Hydraulic Conductivity and Pore Connectivity. Effects of Conventional and No-till Systems Determined Using a Simple Laboratory Device. *Geoderma* **2019**, *337*, 1236–1244. [CrossRef]
22. International Union of Soil Sciences (IUSS) Working Group WRB. *International Soil Classification System for Naming Soils and Creating Legends for Soil Maps*, 4th ed.; IUSS: Vienna, Austria, 2022; ISBN 9798986245119.
23. ISO 11464:1994; Soil Quality—Pretreatment of Samples for Physico-Chemical Analyses. ISO: Geneva, Switzerland, 1994. Available online: <https://www.iso.org/standard/19415.html> (accessed on 29 June 2022).
24. ISO 11277:1998; Soil Quality—Determination of Particle Size Distribution in Mineral Soil Material—Method by Sieving and Sedimentation. ISO: Geneva, Switzerland, 1998. Available online: <https://www.iso.org/standard/19255.html> (accessed on 29 June 2022).
25. ISO 10390:2005; Soil Quality—Determination of PH. ISO: Geneva, Switzerland, 2005. Available online: <https://www.iso.org/standard/40879.html> (accessed on 29 June 2022).
26. ISO 11265:1994/Cor 1:1996; Soil Quality—Determination of the Specific Electrical Conductivity—Technical Corrigendum 1. ISO: Geneva, Switzerland, 1996. Available online: <https://www.iso.org/standard/26684.html> (accessed on 29 June 2022).
27. ISO 14235:1998; Soil Quality—Determination of Organic Carbon by Sulfochromic Oxidation. ISO: Geneva, Switzerland, 1998. Available online: <https://www.iso.org/standard/23140.html> (accessed on 29 June 2022).
28. Schindler, U.G.; Müller, L. Soil Hydraulic Functions of International Soils Measured with the Extended Evaporation Method (EEM) and the HYPROP Device. *Open Data J. Agric. Res.* **2017**, *3*, 1–7. [CrossRef]
29. Haghverdi, A.; Öztürk, H.S.; Durner, W. Measurement and Estimation of the Soil Water Retention Curve Using the Evaporation Method and the Pseudo Continuous Pedotransfer Function. *J. Hydrol.* **2018**, *563*, 251–259. [CrossRef]

30. Campbell, G.; Campbell, C.; Cobos, D.; Crawford, L.B.; Rivera, L.; Chambers, C. *Operation Manual for HYPROP*; UMS: Munich, Germany, 2015.
31. Pertassek, T.; Peters, A.; Durner, W.; Data, H.; Software, E.; Durner, W. *HYPROP Data Evaluation Software*; UMS: Munich, Germany, 2011; pp. 1–47.
32. van Genuchten, M.T. A Closed-Form Equation for Predicting the Hydraulic Conductivity of Unsaturated Soils. *Soil Sci. Soc. Am. J.* **1980**, *44*, 892–898. [[CrossRef](#)]
33. Mualem, Y. A New Model for Predicting the Hydraulic Conduc. *Water Resour. Res.* **1976**, *12*, 513–522. [[CrossRef](#)]
34. Zhang, R. Determination of Soil Sorptivity and Hydraulic Conductivity from the Disk Infiltrometer. *Soil Sci. Soc. Am. J.* **1997**, *61*, 1024–1030. [[CrossRef](#)]
35. Defterdarović, J.; Filipović, L.; Kranjčec, F.; Ondrašek, G.; Kikić, D.; Novosel, A.; Mustać, I.; Krevh, V.; Magdić, I.; Rubinić, V.; et al. Determination of Soil Hydraulic Parameters and Evaluation of Water Dynamics and Nitrate Leaching in the Unsaturated Layered Zone: A Modeling Case Study in Central Croatia. *Sustainability* **2021**, *13*, 6688. [[CrossRef](#)]
36. Shahgholi, G.; Jnatkhah, J. Investigation of the Effects of Organic Matter Application on Soil Compaction. *Yuz. Yil Univ. J. Agric. Sci.* **2018**, *28*, 175–185. [[CrossRef](#)]
37. Nawaz, M.F.; Bourrié, G.; Trolard, F. Soil Compaction Impact and Modelling. A Review. *Agron. Sustain. Dev.* **2013**, *33*, 291–309. [[CrossRef](#)]
38. Liu, Y.; Cui, Z.; Huang, Z.; López-Vicente, M.; Wu, G.L. Influence of Soil Moisture and Plant Roots on the Soil Infiltration Capacity at Different Stages in Arid Grasslands of China. *Catena* **2019**, *182*, 104147. [[CrossRef](#)]
39. Vereecken, H.; Weihermüller, L.; Assouline, S.; Šimůnek, J.; Verhoef, A.; Herbst, M.; Archer, N.; Mohanty, B.; Montzka, C.; Vanderborght, J.; et al. Infiltration from the Pedon to Global Grid Scales: An Overview and Outlook for Land Surface Modeling. *Vadose Zone J.* **2019**, *18*, 1–53. [[CrossRef](#)]
40. Guo, X.; Fu, Q.; Hang, Y.; Lu, H.; Gao, F.; Si, J. Spatial Variability of Soil Moisture in Relation to Land Use Types and Topographic Features on Hillslopes in the Black Soil (Mollisols) Area of Northeast China. *Sustainability* **2020**, *12*, 3552. [[CrossRef](#)]
41. Magdić, I.; Safner, T.; Rubinić, V.; Rutić, F.; Husnjak, S.; Filipović, V. Effect of Slope Position on Soil Properties and Soil Moisture Regime of Stagnosol in the Vineyard. *J. Hydrol. Hydromech.* **2022**, *70*, 62–73. [[CrossRef](#)]
42. Weninger, T.; Filipović, V.; Mešić, M.; Clothier, B.; Filipović, L. Estimating the Extent of Fire Induced Soil Water Repellency in Mediterranean Environment. *Geoderma* **2019**, *338*, 187–196. [[CrossRef](#)]
43. Cleophas, F.; Isidore, F.; Musta, B.; Mohd Ali, B.N.; Mahali, M.; Zahari, N.Z.; Bidin, K. Effect of Soil Physical Properties on Soil Infiltration Rates. *J. Phys. Conf. Ser.* **2022**, *2314*, 012020. [[CrossRef](#)]
44. Dos Santos, K.F.; Barbosa, F.T.; Bertol, I.; De Souza Werner, R.; Wolschick, N.H.; Mota, J.M. Study of Soil Physical Properties and Water Infiltration Rates in Different Types of Land Use. *Semin. Agrar.* **2018**, *39*, 87–98. [[CrossRef](#)]
45. Bayad, M.; Chau, H.W.; Trollove, S.; Moir, J.; Condron, L.; Bouray, M. The Relationship between Soil Moisture and Soil Water Repellency Persistence in Hydrophobic Soils. *Water* **2020**, *12*, 2322. [[CrossRef](#)]
46. Bu, C.F.; Wu, S.F.; Yang, K.B. Effects of Physical Soil Crusts on Infiltration and Splash Erosion in Three Typical Chinese Soils. *Int. J. Sediment Res.* **2014**, *29*, 491–501. [[CrossRef](#)]
47. Güntner, A.; Bronstert, A. Representation of Landscape Variability and Lateral Redistribution Processes for Large-Scale Hydrological Modelling in Semi-Arid Areas. *J. Hydrol.* **2004**, *297*, 136–161. [[CrossRef](#)]
48. Scaini, A.; Audebert, M.; Hissler, C.; Fenicia, F.; Gourdol, L.; Pfister, L.; Beven, K.J. Velocity and Celerity Dynamics at Plot Scale Inferred from Artificial Tracing Experiments and Time-Lapse ERT. *J. Hydrol.* **2017**, *546*, 28–43. [[CrossRef](#)]
49. Goebel, M.O.; Bachmann, J.; Reichstein, M.; Janssens, I.A.; Guggenberger, G. Soil Water Repellency and Its Implications for Organic Matter Decomposition—Is There a Link to Extreme Climatic Events? *Glob. Change Biol.* **2011**, *17*, 2640–2656. [[CrossRef](#)]
50. Jiang, Z.Y.; Li, X.Y.; Wei, J.Q.; Chen, H.Y.; Li, Z.C.; Liu, L.; Hu, X. Contrasting Surface Soil Hydrology Regulated by Biological and Physical Soil Crusts for Patchy Grass in the High-Altitude Alpine Steppe Ecosystem. *Geoderma* **2018**, *326*, 201–209. [[CrossRef](#)]
51. Zhang, Y.; Zhang, Z.; Ma, Z.; Chen, J.; Akbar, J.; Zhang, S.; Che, C.; Zhang, M.; Cerdà, A. A Review of Preferential Water Flow in Soil Science. *Can. J. Soil Sci.* **2018**, *98*, 604–618. [[CrossRef](#)]

**Disclaimer/Publisher’s Note:** The statements, opinions and data contained in all publications are solely those of the individual author(s) and contributor(s) and not of MDPI and/or the editor(s). MDPI and/or the editor(s) disclaim responsibility for any injury to people or property resulting from any ideas, methods, instructions or products referred to in the content.